Carbohydrate Polymers 90 (2012) 551–557

Contents lists available at SciVerse ScienceDirect

Carbohydrate Polymers

journal homepage: www.elsevier.com/locate/carbpol

A phenomenological and thermodynamic study of the water permeation process in corn starch/MMT films

Aníbal M. Slavutsky[a,*], María A. Bertuzzi[b]

[a] Agencia Nacional de Promoción Científica y Tecnológica (ANPCyT), CIUNSa, Universidad Nacional de Salta, Av. Bolivia 5150, A4408TVY, Salta, Argentina
[b] Instituto de Investigaciones para la Industria Química (CONICET), CIUNSa, Facultad de Ingeniería, Universidad Nacional de Salta, Av. Bolivia 5150, A4408TVY, Salta, Argentina

ARTICLE INFO

Article history:
Received 7 January 2012
Received in revised form 8 March 2012
Accepted 22 May 2012
Available online 30 May 2012

Keywords:
Starch/MMT film
Sorption isotherms
Permeability
Thermodynamic parameters

ABSTRACT

Water transport in edible films of starch based products is a complex phenomenon due to the strong interaction of sorbed water molecules with the polymeric structure of starch. Moisture sorption isotherms of starch and starch/MMT films were obtained. The results indicated that nanoclay incorporation produces a decrease of water uptake at all temperatures analysed. Thermodynamic parameters showed that sorption process is less favourable when MMT is incorporated into the starch matrix. Effect of driving force and water activity (a_w) values at each side of the film on permeability and diffusivity coefficients were analysed. The effect of the tortuous pathway generated by MMT incorporation was significant only in the middle and lower range of a_w. At high a_w range the plasticizing effect of water dominated and MMT incorporation had little effect on the water barrier properties of these films.

1. Introduction

Polysaccharides such as starch, cellulose derivates and plant gums have been reported as edible films and coatings in food packaging and preservation (Kester & Fennema, 1986). Generally, the main functional properties of these hydrophilic materials strongly depend on their water content and therefore on the surrounding humidity. The relationship between a_w and moisture content is described by moisture sorption isotherms. Water acts as a plasticizer for hydrophilic materials whose mechanical and barrier properties depend strongly on water content (Bertuzzi, Armada, & Gottifredi, 2003).

The mechanics for and the predictions of water transport through hydrophilic films are extremely complex. The complexity is due to nonlinear behaviour of water sorption isotherms and the water content dependency of diffusivity at water activities higher than 0.55. Water vapour transmission rate of hydrophilic films varies nonlinearly with water vapour pressure (Wiles, Vergano, Barron, Bunn, & Testin, 2000) at water activities higher than 0.55. At lower water activities, Wiles et al. (2000) and Debeaufort, Voilley, and Meares (1994) reported a linear dependence of water vapour transmission rate with water vapour pressure. Larotonda, Matsui, Sobral, and Laurindo (2005) and Müller, Yamashita, and Borges Laurindo (2008) investigated the influence of diffusion coefficient (D_{eff}), water vapour permeability (P) and solubility coefficient of water (β) in different materials. The β value, termed the film hydrophilicity, can be calculated from the first derivative of the water sorption isotherm (represented by GAB model) in relation to a_w, divided by the water vapour pressure (p_w) at the sorption isotherm temperature. The average β values for each range were determined and represented by β'. Water vapour permeability can be obtained using ASTM E96method (Bertuzzi, Castro Vidaurre, Armada, & Gottifredi, 2007). The diffusivity coefficient is obtained from the solubility and permeability coefficients assuming that Henry's law and Fick's first law fully apply (Larotonda et al., 2005).

Nanotechnology focuses on the characterization, fabrication and manipulation of biological and nonbiological structures smaller than 100 nm. The design of internal structures of microscale or nanoscale can improve the functional properties, morphology and stability of the polymer matrix used in edible films and coatings (Azeredo, 2009). Nanocomposites are hybrid nanostructured materials. One of the most studied nanoclay raw materials is montmorillonite (MMT) a 2:1 layered smectite clay mineral with a plate structure. Montmorillonite consists of 1 nm thick aluminosilicate layers surface-substituted with metal cations and stacked in 10 μm-sized multilayer stacks. Naturally occurring MMT is hydrophilic (Alexandre & Dubois, 2000). Nanoclay and starch can interact in different manners depending on nanoclay dispersion in the polymer matrix. Micro or nanocomposites can be formed. In microcomposites, polymer and clay remain immiscible (phase separation), resulting in agglomeration of the clay in the matrix and poor macroscopic properties of the material.

* Corresponding author at: Instituto de Investigaciones para la Industria Química (CONICET), CIUNSa, Universidad Nacional de Salta, Av. Bolivia 5150, A4408TVY, Salta, Argentina. Tel.: +54 387 4255410; fax: +54 387 4251006.
E-mail address: amslavutsky@gmail.com (A.M. Slavutsky).

0144-8617/$ – see front matter © 2012 Elsevier Ltd. All rights reserved.
http://dx.doi.org/10.1016/j.carbpol.2012.05.077

Interaction between layered silicates and polymer chains may produce two types of nanoscale composites. The intercalated nanocomposites result from the penetration of polymer into the interlayer region of the clay, resulting in an ordered multilayer structure with alternating polymer/inorganic layers at a repeating distance of a few nanometers. The exfoliated nanocomposites involve extensive polymer penetration, with the clay layers delaminated and randomly dispersed in the polymer matrix (Azeredo, 2009). X-ray diffraction provides indication of the overall degree of intercalation/exfoliation (Tjong, 2006). Several authors studied the effects of MMT incorporation on the properties of hydrophilic films such as permeability, mechanical properties, moisture sorption isotherms, etc. (Almasi, Ghanbarzadeh, & Entezami, 2010; Cyras, Manfredi, Ton-That, & Vázquez, 2008; Dean, Yu, & Wu, 2007; Majdzadeh-Ardakani, Navarchian, & Sadeghi, 2010; Ning, Xingxiang, Na, & Shihe, 2009; Tunc et al., 2007; Tunç & Osman, 2010).

However, the study of the thermodynamic parameters of the water sorption process in starch/MMT nanocomposite films, and the effect on the water permeation process of the humidity gradient at which the film was exposed, have not been reported yet.

The aims of this work were to study the nature of water sorption process based on thermodynamic analysis and investigate the effect of humidity gradient (driving force) on water vapour permeability of starch/MMT nanocomposite films.

2. Materials and methods

2.1. Materials

Commercial and food grade corn starch (Unilever, Argentina) was used as polymeric matrix for film formulation. Glycerol (Mallinckrodt, USA) was added as a plasticizer. Montmorillonite (MMT) nanoclay was obtained from Minarco S.A. (Buenos Aires, Argentina). The sample was homogenized by sieving in 200-mesh (ASTM). Ethylene glycol (Mallinckrodt, USA) was used for density determinations. P_2O_5 (Mallinckrodt, USA) was used as desiccant and saturated solution of $Mg(NO_3)_2$ (Mallinckrodt, USA) and NaCl (Mallinckrodt, USA) was used to obtain a relative humidity of 53% and 75%, respectively.

2.2. Preparation of MMT solution

MMT solution was prepared stirring nanoclay and water (1.5%, w/v) during 3 h at 80 °C. The suspension was centrifuged at 2500 rpm. Insoluble matter was rejected. The larger particles or aggregates of nanoclay constituted the precipitate. The smaller particles of MMT remained in colloidal solution and were separated with the liquid phase. Centrifugation was used as a selective method of separation. Montmorillonite concentration of MMT solution was determined by drying a 20 mL aliquot in an oven at 105 °C.

2.3. Film preparation

Film-forming solution was prepared by mixing starch, glycerol in a concentration of 20% (w/w) of starch, water and the addition of an appropriate amount of MMT solution (prepared as was described in Section 2.2) to obtain a MMT concentration of 5% (w/w) of starch. The resulting dispersion was kept 60 min in an ultrasonic bath. Dispersions were gelatinized in a shaker water bath at 78–80 °C for 10 min. This procedure ensured disintegration of starch granules and formation of a homogeneous dispersion. The resulting dispersion, while still hot, was poured on polystyrene plates. Then, they were placed in an air-circulating oven at 35 °C and 53% RH for 15 h. After that, plates were removed from the oven and films peeled off.

2.4. Determination of moisture sorption

Constant relative humidity environments were established inside sorbostats, glass jars, using salt solutions. The salts used (LiCl, CH_3COOK, $MgCl_2$, K_2CO_3, $Mg(NO_3)_2$, NaBr, NaCl, KCl) were the different salts recommended by the European project COST-90 (Spiess & Wolf, 1983), to cover a water activity (a_w) range from 0.10 to 0.90. Film samples (rectangular strips approximately 2 cm^2 area) were first freeze-dried (Thermovac Industries Corp., USA) and stored in a desiccator with P_2O_5 during 48 h. Samples were weighed and placed on a stainless plastic lattice by holding it on a tripod inside the sorbostats that contain the saturated salt solutions and then the sorbostats were sealed. The sorbostats were kept inside an environmental chamber maintained at constant temperature. Film samples were equilibrated in the sorbostats for 4 days before their weights were recorded. The weights of the samples were checked during 3 days more. Equilibrium was judged to have been attained when the difference between two consecutive sample weightings was less than 1 mg/g dry solid. Data were reported for each relative humidity as gram of water sorbed/100 g dry film. Absorption tests were done in quadruplicate at each a_w. The moisture sorption determination was done at 5, 25, 35 and 45 °C.

The data obtained were fitted by GAB sorption model, as described by Eq. (1):

$$w_e = \frac{w_0 \cdot C \cdot k \cdot a_w}{(1 - k \cdot a_w)(1 - k \cdot a_w + C \cdot k \cdot a_w)} \quad (1)$$

where w_e is the equilibrium moisture content (g water/100 g dry film), w_0 is the monolayer content (g water/100 g dry film), C is Guggenhein constant related to sorption heat monolayer, and k is a correction factor related to sorption heat multilayer.

The quality of the fitting was evaluated through the R^2 and through the mean relative percent error (%E) defined as:

$$\%\ \text{error} = \sum_{n=1}^{n} \left[\left| \frac{w_{e,i} - w_{p,i}}{w_{e,i}} \right| \right] \times \frac{100}{n} \quad (2)$$

where n is the number of data points, w_e and w_p are experimentally observed and predicted by the model values of the equilibrium moisture content, respectively. The mean relative percentage error (%E) has been widely adopted throughout the literature to evaluate the goodness of fit of sorption models, with a %E value below 10% indicative of a good fit for practical applications (Al-Muhtaseb, McMinn, & Magee, 2002).

2.5. Determination of thermodynamic parameters

The neat isosteric heat of sorption (Q_{st}) provides an indication of the binding energy of water molecules and has some bearing on the energy balance of drying operation (Iglesias & Chirife, 1982). It is defined as the difference between the actual enthalpy change of sorption at constant moisture sorption, w_e, isosteric heat of sorption (ΔH), and latent heat of water condensation (λ):

$$Q_{st}|_{w_e} = \Delta H - \lambda \quad (3)$$

These values can be deduced from the sorption isotherm data at a number of temperatures by applying Clausius–Clapeyron equation:

$$\frac{\Delta H}{R} = \frac{\partial \ln p}{\partial (1/T)} \quad (4)$$

where p is the water vapour pressure (a_w multiplied by water pure vapour pressure at temperature isotherm), T is the absolute temperature and R is the universal gas constant. The relation is applied to the system and the pure water whit the following assumptions:

(1) the heat of vaporization of pure water and excess heat of sorption do not change with temperature and (2) the moisture content of the system remains constant (Al-Muhtaseb et al., 2002).

Gibb's energy changes (ΔG) were calculated as follows:

$$\Delta G = R \cdot T \cdot \ln a_w \tag{5}$$

and entropy changes of sorption process (ΔS) can be calculated from Gibb's equation as suggested by:

$$\Delta S = \frac{\Delta H - \Delta G}{T} \tag{6}$$

2.6. Density

Film density was determined by pycnometry (Displacement Method). Due to high solubility of starch films in water, ethylene glycol was used. The weak ethylene glycol/starch affinity ensures the non-penetration of ethylene glycol in the film matrix. The initial dry matter of each film was obtained after drying film specimens in desiccators containing P_2O_5 during a week. Measurements were performed by triplicate. Density was calculated as follows:

$$\rho = \frac{m_p}{V_m} \tag{7}$$

where ρ is the density (g/cm^3), m_p (g) is the weight of film and V_m (cm^3) is volume of film.

2.7. Water vapour permeability

The apparatus and methodology described in the ASTM E96(ASTM, 2000) were used to measure film permeability. Film specimens were conditioned for 48 h in a chamber at 25 °C and 53% relative humidity ($Mg(NO_3)_2$ saturated salt solution) before being analysed. Films were sealed on cups containing different saturated salt solution or distilled water that provides higher relative humidity. Test cups were placed in a desiccator cabinet maintained at constant temperature. Saturated salt solutions were used to provide specific relative humidity. In all cases, relative humidity inside desiccator cabin was lower than relative humidity inside the cups. Table 2 shows the range of a_w used in each assay. A fan was used to maintain uniform conditions at all test locations over the specimen. Weight loss measurements were taken by continuous weighing of the test cup to the nearest 0.001 g with an electronic scale (Ohaus PA313, USA). Data were transferred to a computer. Weight loss was plotted over time and when steady state (straight line) was reached, 8 h more were registered. Thickness value was the mean value of five measurements and it was used for water vapour permeability calculations. The water vapour transmission rate (WVTR) was calculated from the slope (G) of a linear regression of weight loss versus time (Eq. (8)) and measured water vapour permeability (P) was calculated according to Eq. (9):

$$\mathrm{WVTR} = \frac{G}{A} \tag{8}$$

$$P = \mathrm{cte} \cdot \frac{\mathrm{WVTR} \cdot l}{p_{w0} - p_{w2}} \tag{9}$$

Corrected values of water vapour permeability (P_c) were obtained according the equations proposed by Gennadios, Weller, and Gooding (1994):

$$P_c = \mathrm{cte} \cdot \frac{\mathrm{WVTR} \cdot l}{\Delta p_r} \tag{10}$$

$$\Delta p_r = p_{w1} - p_{w2} \tag{11}$$

$$p_{w1} = p_T - (p_T - p_{w0})\exp^{(N_w \cdot h_i / c \cdot D)} \tag{12}$$

where l is the film thickness, A is the area of exposed film, p_{w1} is partial pressure of water vapour at underside of film (Pa), p_T is total atmospheric pressure (Pa), p_{w2} is partial pressure of water vapour at the film surface outside the cup (Pa), p_{w0} is partial pressure of water vapour in air at the surface of distilled water or saturated solution, N_w is measured value of water vapour transmission rate (g/mol cm^2 s) from surface of distilled water or saturated salt solution to the internal surface of the film (air gap resistance), h_i is air gap between film and surface of distilled water or saturated salt solution in the cup (cm), c is total molar concentration of air and water vapour (g/mol cm^3), D is diffusivity of water vapour in air (cm^2/s) and cte is a constant to satisfies unit conversions. % error was calculated as follows:

$$\%\ \mathrm{error} = \frac{P_c - P}{P_c} \cdot 100 \tag{13}$$

2.8. Solubility coefficient of water in the film

The solubility coefficient of water was determined according of first derivate of GAB model divided by p_w, based on the experimental data of water sorption isotherm:

$$\beta = \frac{C \cdot k \cdot w_0}{p_w} \left\{ \frac{1}{(1 - k \cdot a_w) \cdot (1 - k \cdot a_w + C \cdot k \cdot a_w)} - \frac{a_w}{[(1 - k \cdot a_w) \cdot (1 - k \cdot a_w + Ck \cdot a_w)]^2} \cdot [-k \cdot (1 - k \cdot a_w + C \cdot k \cdot a_w) + (1 - k \cdot a_w) \cdot (-k + C \cdot k)] \right\} \tag{14}$$

The coefficient of water diffusion through the film was determined from P_c, β and ρ values considering that Henry's law fully apply. The β' value used to determined the diffusion coefficient, in each case, was the median of a_w range used in permeability measurement:

$$D_{eff} = \frac{P_c}{\beta' \cdot \rho} \tag{15}$$

2.9. X-ray diffraction (XRD)

X-ray diffraction spectra were carried out on a diffractometer Rigaku Mini Flex (Japan), using a Cu Kα radiation, 40 kV and 20 mA over an angular range 1–40° with step size 0.02. Samples were previously conditioned at a relative humidity of 53% and 25 °C were previously conditioned at 53% RH and 25 °C.

2.10. Statistical analysis

Statistics on a completely randomized design were performed with the analysis of variance (ANOVA) procedure in Graph Pad Prism 5.01 software. Tukey's multiple range test ($p \leq 0.05$) was used to detect differences among mean values of films properties.

3. Results and discussion

3.1. Moisture sorption isotherm

Fig. 1 shows moisture sorption isotherm data obtained at 25 °C for starch and starch/MMT films. Sorption curves correspond to a typical of water sensitive polymers and sorption levels were within the range reported for starch films (Kampeerapappun, Ahtong, Pentrakoon, & Srikulkit, 2007; Müller, Laurindo, & Yamashita, 2011). Curves present a relative slight slope at low values of a_w, but take an exponential course at high relative humidities (above 0.60). The structure of the film is modified above a certain degree of freedom of water. Under these conditions, polymeric chains swell altering its structure. Experimental data obtained for starch/MMT film indicate that incorporation of nanoclay reduced water sorption. This effect increases for high a_w, demonstrating that water

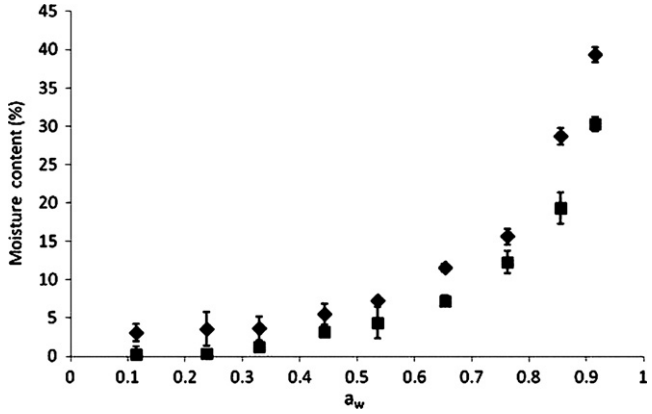

Fig. 1. Moisture sorption isotherm of starch (♦) and starch/MMT (■) films at 25 °C.

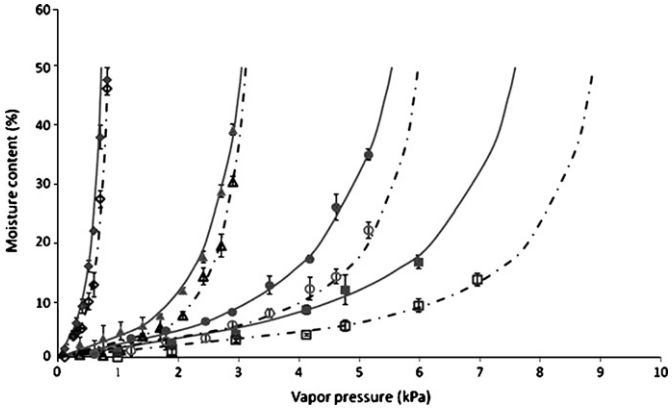

Fig. 2. Moisture sorption isotherm of starch (—) and starch/MMT (– · –) films at different temperatures and GAB model (starch: (♦) 5 °C; (▲) 25 °C; (●) 35 °C; (■) 45 °C; starch/MMT: (◊) 5 °C; (△) 25 °C; (○) 35 °C; (□) 45 °C).

has less affinity with the film. MMT is capable to interact with hydrophilic group of starch. These results indicated that the addition of MMT improves the water resistance of the starch matrix. Almasi et al. (2010) justified this kind of findings postulating that starch forms hydrogen bonds with the hydroxyl groups of the MMT layers, and this strong structure could reduce the diffusion of water molecules in the material.

The effect of water vapour pressure on moisture content of starch and starch/MMT films at different temperatures is shown in Fig. 2. The fits of GAB model are also shown. The increase of temperature decreases the adsorption of water on films. Water adsorption of starch/MMT films is lower than water sorption of starch films at all temperatures tested. Sorption and mixing processes are exothermic since the moisture content decreases with temperature at a given value of a_w (data not shown).

Table 1
Estimated GAB parameters for starch and starch/MMT films.

Temperature (°C)	w_0	C	k	R^2	% error
Starch					
5	13.26	0.9301	0.9650	0.96	4.37
25	11.72	0.7031	0.8543	0.98	1.68
35	11.05	0.9830	0.8320	0.97	2.15
45	7.04	1.8054	1.1000	0.97	2.53
Starch/MMT					
5	10.31	0.8162	0.8896	0.99	0.97
25	8.10	0.4728	0.8922	0.97	2.58
35	5.03	1.8808	0.8520	0.98	1.21
45	4.35	1.9763	0.9900	0.99	1.63

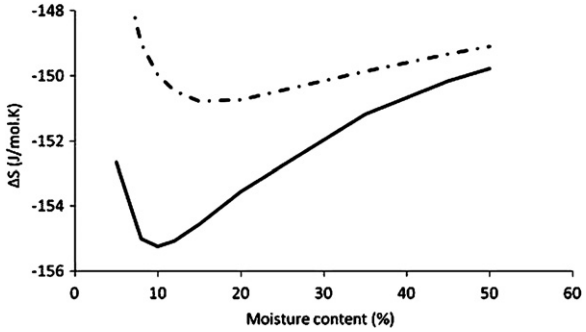

Fig. 3. Change entropy for of starch (– · –) and starch/MMT (—) films.

Table 1 shows the GAB model parameters obtained for starch films and starch/MMT films. Water monolayer values decrease with temperature indicating an exothermic process. Starch/MMT films presented monolayer values lower than starch film. This indicates that MMT reduce the site number where water molecules can interact with starch chains, decreasing the adsorption of water in the films. *C* parameters indicate that all isotherms correspond to type III according to Brunauer classification. These isotherms are observed when liquid or vapour acts as a strong solvent or swelling agent for the polymers (Bertuzzi et al., 2003).

3.2. Thermodynamic parameters

The entropy changes, Gibb's energy changes and isosteric heats of sorption were calculated using Eqs. (3), (4), (5) and (6). Fig. 3 shows entropy changes for starch films and starch/MMT films. The entropy curve exhibits a well-defined minimum corresponding to the completion of the monolayer. The decrease in entropy is associated with loss of mobility of water molecules followed by an increase in entropy as water recovers mobility by forming several layers (Al-Muhtaseb, McMinn, & Magee, 2004; Bertuzzi et al., 2003). Starch/MMT films presented entropy changes values smaller than starch films, indicating that structure is more stable. At low moisture content a marked difference between both curves is observed suggesting that the interaction between water and starch/MMT films is stronger than between water and starch films. At high moisture content the two curves are similar. The process of water sorption is clearly irreversible because a net entropy production is observed along the whole process. Almost constant entropy can be observed at high moisture contents suggesting that desorption is reversible until a critical moisture content is reached.

Fig. 4 shows the values obtained for Gibb's energy changes and isosteric heats of sorption. The values obtained for Gibb's energy

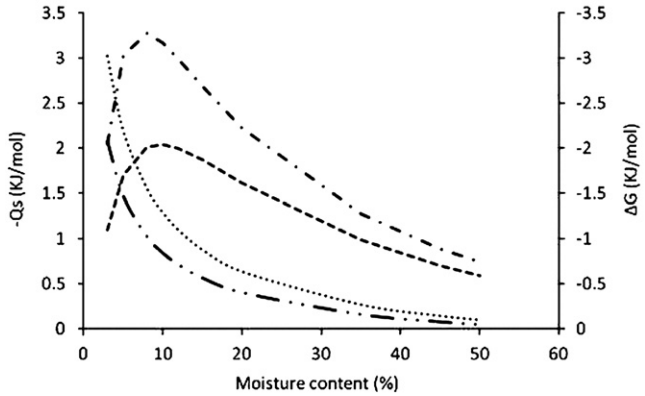

Fig. 4. Gibb's energy changes for starch (···) and starch/MMT (—··—) films. Net isosteric heats of sorption for starch (- - -) and starch/MMT (– · –) films.

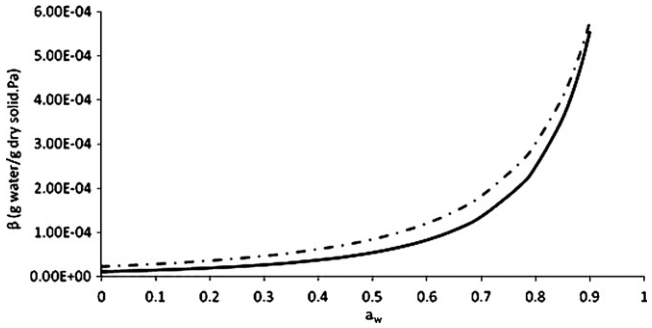

Fig. 5. Water solubility coefficients of starch (– · –) and starch/MMT (—) films.

changes for both samples were negative as it was expected for a spontaneous process. In addition, the starch film presented lower values (greater in absolute values) than starch/MMT films suggesting that the process occurs with more energy liberation, which indicate that adsorption is a more favourable process in starch films. The difference between curves decreases as the moisture content increases.

The heat of adsorption is a measure of the energy released on sorption (the heat of adsorption is negative) (Al-Muhtaseb et al., 2002). Water sorption process in starch based films is exothermic, within the range of water activities investigated. Values of net isosteric heat of sorption have been deduced from water isotherm data, adopting the Clausius–Clapeyron equation. As water vapour is brought in contact with a heterogeneous surface, where active sites of different energy are present, the most active sites are those first sorbed by the water molecules followed by those less active until the first layer of water is completed (Bertuzzi et al., 2003). Starch films and starch/MMT films present a peak at similar monolayer values obtained by GAB model. These indicate that the completion of the monolayer is accomplished with liberation of energy. In starch/MMT films this liberation is greater than in starch films, indicating that formation of the monolayer is less favourable. Until the monolayer is completed, net isosteric heat of sorption increases with moisture content at the same times as multilayer is formed. The formation of multilayer for starch/MMT films seems to be more pronounced with the increase of moisture content. That occurs because the water competes with MMT for OH-groups of starch, and at high moisture content, this process is favoured as it is observed in the curves of Gibb's energy change.

3.3. Density

Film density increases with the incorporation of MMT. This is explained by the high density of clay (2.60 g cm^{-3}). Density of starch films is 1.32 ± 0.04 g cm^{-3} and starch/MMT films presented a density value of 1.53 ± 0.05 g cm^{-3}. Results were similar to the values reported by Müller et al. (2011).

3.4. Water vapour permeability, solubility and diffusion coefficient

Fig. 5 shows the water solubility coefficients as a function of water activity for starch films and starch/MMT films. At low values of a_w solubility remains practically constant, but there is an exponential increase from 0.6 for both kind of films. This inflexion point corresponds to the completion of the monolayer as can be seen in Fig. 1 and Table 1. After 0.6, water molecules recover mobility and solubility of water in the film increases notoriously. The difference between solubility of starch films and starch/MMT films is greater in the range of $a_w = 0.55$–0.75, showing the benefit of MMT incorporation in the starch matrix. MMT acts delaying plasticizer effect of water on film due to the high interaction between OH-groups of starch and MMT. At the same time, as a_w increases, values of the solubility coefficient in both film approaches. Similar results were obtained for Müller et al. (2011).

Permeability determinations are based on measuring the flow of water vapour through a film submitted for a particular water vapour pressure gradient. However, due to the shape of the sorption isotherm and the changes that occur in the material from $a_w = 0.6$, permeability varies considerably for a same driving force ($\Delta a_w = a_w^{ext} - a_w^{int}$), depending on the values of a_w on each side of the film. Table 2 shows corrected and uncorrected water vapour permeability for the different ranges of a_w used to generate water vapour gradient through the film. % error calculated according to procedure delineated by Gennadios et al. (1994), indicates that at a same value of Δa_w, % error in permeability measurements increases with a_w values at each side of the film. This indicates the importance of data correction to obtain a better understanding of barrier properties of these films. Permeability increases with a_w values at each side of the film when similar driving force (Δa_w) was used. The permeabilities of starch/MMT films are lower than permeabilities values of starch film, except for high a_w values (0.762–1) when no significative differences between films are detected. It indicates that MMT reduces the plasticizing effect of water in the starch film within the a_w range studied, being less significant at high a_w values because of the large change in the material at high moisture contents. The driving force and the a_w at each side of the film play important roles in the permeability process. At high a_w, adsorption of water molecules produces a greater increment on mobility of starch chain and the rupture of interaction between MMT–starch–glycerol. The tortuous pathway produced by MMT gets lost at high a_w range and small driving forces, favouring film permeability. Effect of MMT on water vapour permeability is clearly important when a_w values at each side of the film are lower than 0.80. The obtained results clearly show the effect of non-linearity of the sorption isotherm on the permeation process and explain the dependence of the phenomenological coefficient (permeability) with the driving force (Δa_w).

Diffusion coefficient data provide more information and evidence of MMT effect in the barrier behaviour of the starch matrix. Table 2 shows solubility and diffusivity coefficients obtained by application of Eqs. (14) and (15), respectively. Obtained values indicate that incorporation of MMT reduces D_{eff} of starch film. Diffusivity values obtained at low driving forces are in the same range of those reported by Chivrac, Angellier-Coussy, Guillard, Pollet, and Avérous (2010). At a similar driving force ($\Delta a_w = 0.2$), D_{eff} increases with a_w up to approximately 0.6 and then decreases. This behaviour indicates that water molecules increase free volume, generate relaxing of polymer matrix and improve the adsorption of water molecules in new active sites, producing a reduction of D_{eff}. Incorporation of MMT produces an additional decrease in D_{eff} due to the tortuous pathway formed by the nanoclay.

When driving force is 0.2 and a_w at each side of the film are small there is little difference between solubility of starch films and starch/MMT films, and the divergence in permeability is dependent on D_{eff}. A combined effect is found at a_w middle zone, product of tortuous pathway and less adsorption of water molecules in starch/MMT matrix. That occurs because in this zone the plasticizing effect is more important in starch film. The adsorption of water is greater and produces an increase in the free volume inside the polymer and generates high mobility of water molecules that conduces to a decrease in D_{eff}. At high a_w zone, monolayer has been completed and water has increased mobility. Incorporation of MMT in the film matrix and the tortuous path formed are not obstacles for water transport through the film. The results of P_c and D_{eff} are connected with entropy changes and net isosteric heat of sorption. Figs. 3 and 4 show that at high moisture content occurs the formation of multilayer and the system presents more affinity

Table 2
Phenomenological coefficients of starch films and starch/MMT films.

$a_w^{ext}-a_w^{int}$	$\lvert\Delta a_w\rvert$	P (g/m s Pa)	P_c (g/m s Pa)	% error	β' (g_w/g_{ds} Pa)	D_{eff} (cm^2/s)
Starch						
0.114–0.329	0.215	1.50E−10	1.74E−10	14.13	0.375E−04	3.54E−08
0.329–0.536	0.207	3.74E−10	7.14E−10	47.64	0.673E−04	8.04E−08
0.536–0.762	0.226	4.59E−10	8.02E−10	42.81	1.47E−04	4.15E−08
0.762–1.000	0.238	6.93E−10	18.7E−10	63.13	4.98E−04	2.86E−08
0.000–0.536	0.536	2.00E−10	2.48E−10	19.41	0.427E−04	4.40E−08
0.329–0.762	0.433	3.28E−10	5.03E−10	34.79	1.00E−04	3.82E−08
0.536–1.000	0.464	6.54E−10	12.9E−10	49.59	2.56 -04	3.84E−08
Starch/MMT						
0.114–0.329	0.215	9.10E−11	0.995E−10	8.64	0.204E−04	3.19E−08
0.329–0.536	0.207	2.53E−10	3.89E−10	35.16	0.413E−04	6.17E−08
0.536–0.762	0.226	3.84E−10	6.08E−10	36.96	1.05E−04	3.80E−08
0.762–1.000	0.238	6.55E−10	17.6E−10	62.80	4.60E−04	2.50E−08
0.000–0.536	0.536	7.41E−11	0.798E−10	7.14	0.239E−04	2.19E−08
0.329–0.762	0.433	2.20E−10	3.16E−10	30.36	6.63E−05	3.12E−08
0.536–1.000	0.464	5.09E−10	8.80E−10	42.20	2.04E−04	2.82E−08

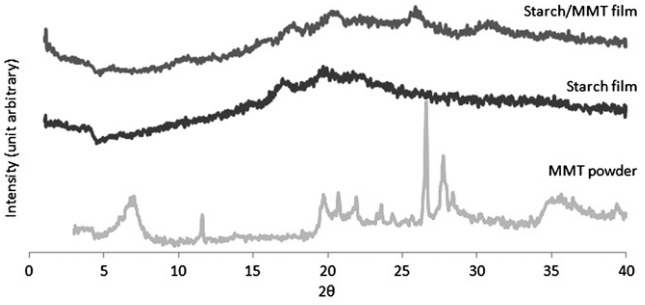

Fig. 6. X-ray diffractograms of starch, starch/MMT films and MMT powder.

by water molecules. This induces changes in film matrix structure and facilitates water permeability.

3.5. X-ray diffraction (XRD)

The results of X-ray diffraction measurements performed on starch films and starch/MMT films as well as on MMT powder are shown in Fig. 6. Starch films present typical patterns, similar to those reported by other authors (Bertuzzi, Armada, & Gottifredi, 2007; Famá, Goyanes, & Gerschenson, 2007). Diffractogram of MMT powder displays an intense diffraction peak at 2θ angle of 7.06° corresponding to a clay inter-layer spacing value of 1.251 nm. Müller et al. (2011) obtained similar X-ray diffraction analyses for MMT. XRD pattern of starch/MMT films shows that the diffraction peak at 2θ angle of 7.06° of MMT disappears. This is indicative of an adequate dispersion of the nanoclay with a high extent of exfoliation in the starch matrix. Huang, Yu, and Ma (2004) and Chivrac et al. (2010) obtain similar results with starch/nanoclay composites. These results confirm that MMT is well distributed in the polymeric matrix, generating a tortuous path for the water molecules that diffuse through the film.

4. Conclusions

Considering the complex mechanisms involved in water vapour transport through starch based films, the effect on permeation process of MMT incorporation was studied through phenomenological and thermodynamic analyses. Water vapour sorption experimental data show an exothermic process and were well described by GAB model. Isotherm curves show an exponential increase of water uptake above $a_w = 0.6$, producing film structural changes which allow a facilitated water transport phenomenon. MMT addition decreases water uptake of starch films in all the studied temperatures. The water content values of the monolayer calculated with GAB equation reduces with MMT incorporation.

Entropy changes and net isosteric heat of sorption show a well-defined peak at monolayer water content and in both cases indicate a more stable and ordered structure when MMT was added. Gibb's energy changes show the process spontaneity and indicate that final structure of starch/MMT films has less affinity to water than films of starch alone.

Permeation process developed in different ranges of a_w (below and above $a_w = 0.6$) evidences modifications of polymer matrix (plasticization by water), showing the influence of driving force and a_w range on permeability (phenomenological coefficient) for these materials. The effect of the tortuous pathway generated by MMT incorporation is significant only at middle and low range of a_w. In the same range of a_w the interactions between OH-groups of starch and MMT were also important. At high a_w range plasticizer effect of water was notorious and MMT incorporation did not have an important effect on the water barrier properties of these films.

Acknowledgements

The authors thank the financial support of Consejo de Investigaciones de la Universidad Nacional de Salta (CIUNSa), Agencia Nacional de Promoción Científica y Tecnológica (ANPCyT) and Instituto de Investigaciones para la Industria Química (INIQUI).

References

Alexandre, M., & Dubois, P. (2000). Polymer-layered silicate nanocomposites: Preparation, properties and uses of a new class of materials. *Materials Science and Engineering R: Reports*, *28*(1–2), 1–63.
Almasi, H., Ghanbarzadeh, B., & Entezami, A. A. (2010). Physicochemical properties of starch–CMC–nanoclay biodegradable films. *International Journal of Biological Macromolecules*, *46*(1), 1–5.
Al-Muhtaseb, A. H., McMinn, W. A. M., & Magee, T. R. A. (2002). Moisture sorption isotherm characteristics of food products: A review. *Food and Bioproducts Processing*, *80*(C2), 118–128.
Al-Muhtaseb, A. H., McMinn, W. A. M., & Magee, T. R. A. (2004). Water sorption isotherms of starch powders. Part 2. Thermodynamic characteristics. *Journal of Food Engineering*, *62*, 135–142.
ASTM. (2000). Standards American Society for Testing and Materials. E96. *Standard test methods for water vapor transmission of materials*. Philadelphia.
Azeredo, H. M. C. D. (2009). Nanocomposites for food packaging applications. *Food Research International*, *42*(9), 1240–1253.
Bertuzzi, M. A., Armada, M., & Gottifredi, J. C. (2003). Thermodynamic analysis of water vapour sorption of edible starch based films. *Food Science and Technology International*, *9*(2), 115–121.
Bertuzzi, M. A., Armada, M., & Gottifredi, J. C. (2007). Physicochemical characterization of starch based films. *Journal of Food Engineering*, *82*(1), 17–25.
Bertuzzi, M., Castro Vidaurre, E., Armada, M., & Gottifredi, J. (2007). Water vapor permeability of edible starch based films. *Journal of Food Engineering*, *80*(3), 972–978.

Chivrac, F., Angellier-Coussy, H., Guillard, V., Pollet, E., & Avérous, L. (2010). How does water diffuse in starch/montmorillonite nano-biocomposite materials? *Carbohydrate Polymers*, *82*(1), 128–135.

Cyras, V. P., Manfredi, L. B., Ton-That, M.-T., & Vázquez, A. (2008). Physical and mechanical properties of thermoplastic starch/montmorillonite nanocomposite films. *Carbohydrate Polymers*, *73*(1), 55–63.

Dean, K., Yu, L., & Wu, D. Y. (2007). Preparation and characterization of melt-extruded thermoplastic starch/clay nanocomposites. *Composites Science and Technology*, *67*(3–4), 413–421.

Debeaufort, F., Voilley, A., & Meares, P. (1994). Water vapour permeability and diffusivity through methylcellulose edible films. *Journal of Membrane Science*, *91*, 125–133.

Famá, L., Goyanes, S., & Gerschenson, L. (2007). Influence of storage time at room temperature on the physicochemical properties of cassava starch films. *Carbohydrate Polymers*, *70*(3), 265–273.

Gennadios, A., Weller, C. L., & Gooding, C. H. (1994). Measurement errors in water vapor permeability of highly permeable, hydrophilic edible films. *Journal of Food Engineering*, *21*(4), 395–409.

Huang, M.-F., Yu, J.-G., & Ma, X.-F. (2004). Studies on the properties of montmorillonite-reinforced thermoplastic starch composites. *Polymer*, *45*(20), 7017–7023.

Iglesias, H. A., & Chirife, J. (1982). *Handbook of food isotherms: Water sorption parameters for food and food components*. New York: Academic Press.

Kampeerapappun, P., Aht-ong, D., Pentrakoon, D., & Srikulkit, K. (2007). Preparation of cassava starch/montmorillonite composite film. *Carbohydrate Polymers*, *67*(2), 155–163.

Kester, J. J., & Fennema, O. R. (1986). Edible films and coatings: A review. *Food Science and Technology*, *40*(12), 47–59.

Larotonda, F. D. S., Matsui, K. N., Sobral, P. J. A., & Laurindo, J. B. (2005). Hygroscopicity and water vapor permeability of Kraft paper impregnated with starch acetate. *Journal of Food and Engineering*, *71*, 394–402.

Majdzadeh-Ardakani, K., Navarchian, A., & Sadeghi, F. (2010). Optimization of mechanical properties of thermoplastic starch/clay nanocomposites. *Carbohydrate Polymers*, *79*, 547–554.

Müller, C. M. O., Laurindo, J. B., & Yamashita, F. (2011). Effect of nanoclay incorporation method on mechanical and water vapor barrier properties of starch-based films. *Industrial Crops and Products*, *33*(3), 605–610.

Müller, C. M. O., Yamashita, F., & Borges Laurindo, J. (2008). Evaluation of the effects of glycerol and sorbitol concentration and water activity on the water barrier properties of cassava starch films through a solubility approach. *Carbohydrate Polymers*, *72*, 82–87.

Ning, W., Xingxiang, Z., Na, H., & Shihe, B. (2009). Effect of citric acid and processing on the performance of thermoplastic starch/montmorillonite nanocomposites. *Carbohydrate Polymers*, *76*, 68–73.

Spiess, W. E. L., & Wolf, W. F. (1983). The results of the COST 90 project on water activity. In *Physical properties of foods*. London: Applied Science Publishers.

Tjong, S. C. (2006). Structural and mechanical properties of polymer nanocomposites. *Materials Science and Engineering*, *53*, 73–197.

Tunc, S., Angellier, H., Cahyana, Y., Chalier, P., Gontard, N., & Gastaldi, E. (2007). Functional properties of wheat gluten/montmorillonite nanocomposite films processed by casting. *Journal of Membrane Science*, *289*(1–2), 159–168.

Tunç, S., & Osman, D. (2010). Preparation and characterization of biodegradable methyl cellulose/montmorillonite nanocomposite films. *Applied Clay Science*, *48*, 414–424.

Wiles, J. L., Vergano, P. J., Barron, F. H., Bunn, J. M., & Testin, R. F. (2000). Water vapor transmission rates and sorption behavior of chitosan films. *Food Engineering and Physical Properties*, *65*(7), 1175–1179.